Modeling the Interference caused to a LoRaWAN Gateway due to Uplink Transmissions

Luis Irio*† and Rodolfo Oliveira*†

*Departamento de Engenharia Electrotécnica, Faculdade de Ciências e Tecnologia (FCT),
Universidade Nova de Lisboa, Caparica, Portugal
†IT, Instituto de Telecomunicações, Portugal
Emails: l.irio@campus.fct.unl.pt, rado@fct.unl.pt

***Abstract*—The performance of Low Power Wide Area Networks (LPWANs), where LoRa networks are included, has spurred much interest in recent times due to the high interest in connecting more and more devices to the so-called Internet of Things (IoT). The massive number of connected devices associated to its random spatial deployment and random network access introduce new degrees of freedom, demanding for innovative performance evaluation approaches. In this paper we study the interference caused to a LoRa gateway due to the uplink transmissions of multiple coexisting LoRa devices. By admitting an uniform spatial distribution of the devices, we show that the aggregate interference caused to a LoRa gateway follows a non-Gaussian distribution and its power can be approximated by a sum of independent non-identical gamma random variables. Our work adopts a typical LoRaWAN operating scenario where the transmissions of LoRa Class A devices are affected by path-loss, shadowing and Rayleigh fading. Numerical results obtained with the modeling methodology are compared with simulation results, and the validation of the proposed model is discussed for different transmission probabilities.**

***Index Terms*—LoRa Networks, Interference Modeling, Performance Evaluation.**

I. Introduction

The necessity of connecting billions of devices to the so-called Internet of Things (IoT) has led to several standardization initiatives and proprietary protocols. Despite of the high number of radio access technologies already available to support wideband data communications (e.g. WiFi, GPRS, 3G, 4G, etc.), it is widely agreed that radio access to IoT networks requires specific protocols particularly tailored to support a massive number of devices that may deployed as necessary. IoT radio access requires the adoption of devices that operate with very low power in order to minimize energy consumption, the devices can operate in a very wide area, and in most of the practical scenarios the transmission rate does not exceed a few tens of kilobits per second. The response to these requirements has been given by the so called Low Power Wide Area Networks (LPWANs) [1], capable of offering affordable low-power devices that operate over very large geographical areas. Contrarily to short-range wireless protocols already proposed for IoT radio access, e.g., Bluetooth, IEEE 802.15.4, LPWANs support long range and low-power operation to a high number of connected devices at the expense of slowing down the transmission rate and increasing latency. Several LPWA technologies have already been proposed. Traditional cellular network operators are currently offering commercial LPWA technologies in licensed bands, e.g. LTE enhancements for Machine Type Communications (eMTC), Extended Coverage GSM (EC-GSM), and Narrow-Band IoT (NB-IoT). Simultaneously, proprietary LPWA technologies, e.g. Sigfox, LoRa, and Ingenu, have gaining interest due to the lower operational costs in non-licensed bands and because they can be deployed at certain areas where no cellular operators are available. In this work we are particularly focused on approaching LoRa due to the rising interest of practitioners, who are currently deploying a global open LoRaWAN network through personal gateways that enable LoRa devices to connect to a decentralized network to exchange data with the applications [2].

LoRa is a proprietary physical layer technology, developed by Semtech Corporation [3], that uses a chirp spread spectrum technique to spread a narrow band signal over a 125, 250 or 500 kHz bandwidth located in a sub-gigahertz unlicensed ISM band. This allows the receiver, usually a gateway, to decode signals a few dBs below the noise floor. The transmission range and the data rate can be also controlled through different Spreading Factors (SF), which vary the receivers' sensivity threshold. LoRaWAN [4] is a medium access control (MAC) protocol designed to run on top of LoRa's modulation. LoRaWAN offers bidirectional communications initiated by the receiver. The communication is initiated by a LoRa device, which sends an uplink message in a random access mode (similar to ALOHA). A LoRa gateway can then respond to the device if the uplink message is successfully received. The devices supporting the bidirectional communication scheme is designated Class A devices.

The performance of LoRa networks has attracted an increasing interest [5]–[8]. Real world indoor and outdoor evaluation campaigns were presented in [5] and [6], respectively. LoRa's scalability was addressed in [7], by considering two capture conditions for the uplink messages. The first condition considered the received Signal-to-Noise Ratio (SNR), while the second one assumed that the uplink message is successfully received whenever its power is 4 times higher than any concurrent transmission. Based on the second capture condition [7] concludes that the interference caused by concurrent uplink transmissions can effectively limit the scalability of LoRa

networks. While [7] considers that LoRa devices adopt the same SF, [8] evaluates the throughput when concurrent upload messages are transmitted with different spreading factors. By considering that a few LoRa devices may use the same SF and the remaining ones can adopt different SFs, [8] derives the network's throughput for different types of SF allocations. When LoRa devices adopt the same SF the capture condition must take into account the interference caused to the gateway by the multiple transmissions. Although LoRa's performance is strongly influenced by the interference caused to the gateway, a detailed study of the interference in such networks is still missing. The transmission of multiple devices without adopting power control origins dominant interferers, i.e. the transmitters more close to the gateway. This fact explains the non-Gaussian distribution of the aggregate interference, making the interference modeling a more difficult exercise.

Motivated by the importance of the interference caused by a massive number of competing LoRa devices, this work characterizes the aggregate interference caused to a LoRa gateway due to the uplink transmissions. We show that the interference power can be approximated by a sum of independent non-identical Gamma random variables. Our work adopts a typical LoRaWAN operating scenario, where LoRa Class A devices transmit with a given probability and are affected by path-loss, shadowing and Rayleigh fading. Numerical and simulation results are compared to evaluate the accuracy of the proposed model. To the best of the authors' knowledge, the presented results are new and can definitely be used as a benchmark for future LoRa performance evaluation studies.

The remainder of this paper is organized as follows. Section II presents the LoRa scenario assumed in our work. Section III describes the steps involved to model the aggregate interference. Section IV compares and discusses numerical and simulation results. Finally, conclusions are presented in Section V.

Notations: In this work, $f_X(.)$ and $M_X(.)$ represent the Probability Density Function (PDF) and the Moment Generating Function (MGF) of a random variable (RV) X, respectively. $\mathrm{P}(X = x)$ is the probability of the RV X. $\Gamma(.)$ represents the complete Gamma function [9]. $K_y(.)$ denotes the modified Bessel function of the second kind with order y [9]. ${}_2\mathrm{F}_1(\cdot,\cdot,\cdot,\cdot)$ represents the Gauss Hypergeometric function [9]. $\mathrm{E}[X]$ and $\mathrm{Var}[X]$ are the expectation and variance of the RV X, respectively.

II. LoRa Network Scenario

We consider a LoRa network scenario where the LoRa devices are spatially deployed in according to a Poisson point process (PPP) with spatial density λ. The devices are distributed over a circular region centered at the gateway, as illustrated in Fig. 1. Since LoRa devices transmit with equal power (no power control is used), the dominant interferers are the ones more close to the gateway due to the non-linearity of the path loss. This have motivated us to divide the circular region in multiple rings (annuli) with the purpose of modeling the interference caused by the devices located within each annulus in a more accurate way. The area of the circular region is given by $A = \pi\left((R_{L+1})^2 - (R_1)^2\right)$, where L represents the number of annuli centered at the gateway with width ρ. R_1 and R_{L+1} represent the inner and outer radius of the circular region. The area of each annulus $l \in L$ is represented by $A_l = \pi\left((R_{l+1})^2 - (R_l)^2\right)$, where $R_{l+1} = (R_l + l\rho)$ and R_l represent the radius of the larger and smaller circles of the annulus l, respectively.

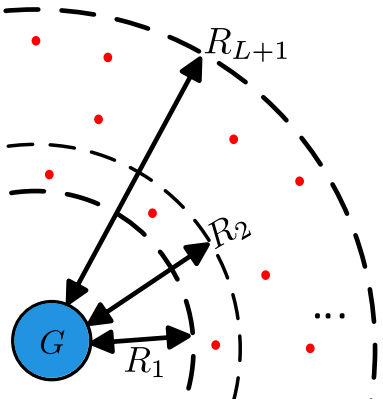

Fig. 1. A LoRa gateway (node G) suffers interference caused by n LoRa devices (red devices).

The number of active LoRa devices located in the annulus $l \in \{1, ..., L\}$ is denoted by the RV X_l. Since the devices are uniformly distributed over the circular region, the probability of finding k active devices located within the annulus l is given by the truncated Poisson distribution as follows

$$P(X_l = k) = \frac{(\lambda A_l \tau)^k e^{-\lambda A_l \tau}}{k! \sum_{i=0}^{n} \frac{(\lambda A_l \tau)^i}{i!} e^{-\lambda A_l \tau}}, 0 \leq k \leq n, \quad (1)$$

where n is the total number of LoRa devices considered in the network. Each device transmits a message with probability τ. Regarding the assumptions related with the radio propagation, we consider that the fading between each device and the gateway is independent and identically distributed (i.i.d). Rayleigh fading and Log-normal shadowing is assumed.

III. Interference caused to LoRa gateway

In this Section we study the interference caused to the gateway by the devices located within a generic annulus l (Subsection III-A). Then we characterize the aggregate interference caused by active LoRa devices located within L annuli and we address the PDF and CDF computation the aggregate interference power.

A. Interference caused by devices positioned at the annulus l

At a given time the interference power received by the LoRa gateway from the active devices positioned at the annulus l is given by $I = \sum_{i=1}^{n_l} I_i$, where I_i is the interference caused by the i-th device, and n_l is the total number of devices positioned at the annulus. I_i is represented by

$$I_i = P_{Tx} \psi_i r_l^{-\alpha}, \quad (2)$$

which takes into account the instantaneous fading and shadowing gain of the channel, between the LoRa gateway and the transmitting device i, ψ_i, the transmitted power[1] of the i-th device, P_{Tx}, the path-loss coefficient, α, and the distance between the i-th device and the LoRa gateway, r_l. Regarding the notation, r_l and ψ_i represent the values of the random variables R_l and Ψ_i, respectively.

Small-scale fading (fast fading) and shadowing (slow fading) gain are represented by the RV Ψ_i. The fast fading gain is assumed to be distributed according to a Rayleigh distribution with PDF

$$f_\zeta(x) = \frac{x}{\sigma_\zeta^2} e^{\frac{-x^2}{2\sigma_\zeta^2}}, \tag{3}$$

where $2\sigma_\zeta^2$ is the average gain (we consider normalized gain, i.e., $2\sigma_\zeta^2 = 1$). The shadowing gain is approximated by a Log-normal distribution

$$f_\xi(x) = \frac{1}{\sqrt{2\pi}\sigma_\xi x} e^{\frac{-(ln(x)-\mu_\xi)^2}{2\sigma_\xi^2}}, \tag{4}$$

where $\sigma_\xi > 0$ and $\mu_\xi = -\frac{\sigma_\xi^2}{2}$ to consider average unitary gain. However, due to the mathematical intractability of Log-normal RV we use a gamma distribution given by

$$f_\xi(x) \approx \frac{1}{\Gamma(\vartheta)} \left(\frac{\vartheta}{\omega_s}\right)^\vartheta x^{\vartheta-1} e^{-x\frac{\vartheta}{\omega_s}}, \tag{5}$$

with $\vartheta = \frac{1}{e^{\sigma_\xi^2}-1}$ and $\omega_s = e^{\mu_\xi}\sqrt{\frac{\vartheta+1}{\vartheta}}$, which can be used to replace the Log-normal distribution in an accurate manner [11]. Finally, the PDF of the fading and shadowing power gain is given by $f_{\Psi_i}(x) \approx f_{\zeta^2}(x) \cdot f_\xi(x)$, that can be simplified to

$$f_{\Psi_i}(x) \approx \frac{2x^{\frac{\vartheta-1}{2}}}{\Gamma(\vartheta)} \left(\frac{\vartheta}{\omega_s}\right)^{\frac{\vartheta+1}{2}} K_{\vartheta-1}\left(\sqrt{\frac{4\vartheta x}{\omega_s}}\right). \tag{6}$$

(6) is the PDF of a Generalized-K distribution [12], which can be approximated by a gamma distribution with scale and shape parameters given by $\theta_\psi = \left(\frac{2(\vartheta+1)}{\vartheta} - 1\right)\omega_s$ and $k_\psi = \frac{1}{\frac{2(\vartheta+1)}{\vartheta}-1}$, respectively [13].

The MGF of the interference caused by the i-th LoRa device positioned over the annulus l, $M_I^i(s)$, with $i = 1, ..., n_l$, is represented as

$$M_I^i(s) = \mathrm{E}_{I_i}[e^{sI_i}] = \mathrm{E}_{\Psi_i}\left[\mathrm{E}_{R_l}[e^{sI_i}]\right]. \tag{7}$$

Because the devices are uniformly spread over the circular regions, the PDF of the distance between the i-th device and the LoRa gateway is given by

$$f_{R_l}(x) = \begin{cases} \frac{2\pi x}{A_l} & R_l < x < R_{l+1}. \\ 0, & \text{otherwise} \end{cases} \tag{8}$$

[1] $P_{Tx} = 14$dBm is assumed [10].

Using (8) and (6), the MGF in (7) is now rewritten as

$$M_I^i(s) = \int_0^{+\infty} \int_{R_i^l}^{R_o^l} e^{sI_i} f_{R_l}(r_l) f_{\Psi_i}(\psi_i)\, dr_l\, d\psi_i, \tag{9}$$

which using (2), (8), k_ψ and θ_ψ, and after solving the integrals, can be written as follows

$$M_I^i(s) = \frac{2\pi}{A_l(2+k_\psi\alpha)(P_{Tx}\theta_\psi s)^{k_\psi}} \cdot \cdot \left(\left(R_o^l\right)^{2+k_\psi\alpha} \varrho(R_o^l) - \left(R_i^l\right)^{2+k_\psi\alpha} \varrho(R_i^l)\right), \tag{10}$$

with

$$\varrho(x) = {}_2\mathrm{F}_1\left(k_\psi, k_\psi + \frac{2}{\alpha}, 1 + k_\psi + \frac{2}{\alpha}, -\frac{x^\alpha}{P_{Tx}\theta_\psi s}\right).$$

Assuming that the interference caused by a LoRa device, I_i, is independent of the other devices and are identically distributed, the MGF of the interference I caused by k devices is the product of the individual MGFs as follows

$$\begin{aligned} M_{I/k}(s) &= M_I^1(s) \times M_I^2(s) \times \cdots \\ &\quad \cdots \times M_I^k(s) = \left(M_I^i(s)\right)^k. \end{aligned} \tag{11}$$

Using the PDF of the interference I caused by the devices located at annulus l,

$$f_I(j) = \sum_{k=0}^{n} f_I(j|X_l = k)\mathrm{P}(X_l = k), \tag{12}$$

the MGF of I can be written as

$$\begin{aligned} \mathrm{E}[e^{sI}] &= \sum_{k=0}^{n} \mathrm{P}(X_l = k) \int_{-\infty}^{+\infty} e^{sj} f_I(j|X_l = k)\, dj \\ &= \sum_{k=0}^{n} \mathrm{P}(X_l = k) M_{I/k}(s) \\ &= \sum_{k=0}^{n} \mathrm{P}(X_l = k) e^{k\, ln(M_I^i(s))} \end{aligned} \tag{13}$$

Replacing (1) in (13), the MGF of I is finally given by

$$\mathrm{E}[e^{sI}] = e^{\beta_l A_l \tau (M_I^i(s)-1)}. \tag{14}$$

At this stage the expectation of the interference caused by the devices located in the l-th annulus can be computed as follows

$$\begin{aligned} \mathrm{E}[I] &= \mathrm{E}\Big[\mathrm{E}\big[I|X_l\big]\Big] = \mathrm{E}\big[I_i\big]\mathrm{E}\big[X_l\big] = \\ &= 2\pi\beta_l\tau P_{Tx} e^{\mu_\xi}\sqrt{e^{\sigma_\xi^2}} \left(\frac{(R_{l+1})^{2-\alpha} - (R_l)^{2-\alpha}}{2-\alpha}\right). \end{aligned} \tag{15}$$

Similarly, the variance of the interference caused by the devices located in the l-th annulus is given by

$$\begin{aligned} \mathrm{Var}[I] &= \mathrm{Var}[I_i]\mathrm{E}[X_l] + \mathrm{E}[I_i]^2\mathrm{Var}[X_l]. \\ &= \pi\beta_l\tau P_{Tx}^2 k_\psi\theta_\psi^2(1+k_\psi) \left(\frac{(R_o^l)^{2-2\alpha} - (R_i^l)^{2-2\alpha}}{1-\alpha}\right). \end{aligned} \tag{16}$$

Previous aggregate interference studies have already considered a circular region as the one considered in this work. It is known that the aggregate interference caused by multiple interferers (uniformly distributed over a circumference) to the node located in the center of the circumference can be approximated by a gamma distribution [14]. Motivated by the fact that the circular region where the LoRa devices are located can be decomposed into multiple annulus, similar to multiple circumferences, we use the method of moments to approximate the distribution of the interference caused by the devices within an annulus trough a gamma distribution. Finally, the parameters (shape (k_l) and scale (θ_l)) of the gamma distribution, that approximate the interference power caused by the LoRa devices located at the annulus l are given by $k_l = \mathrm{E}[I]^2/\mathrm{Var}[I]$, and $\theta_l = \mathrm{Var}[I]/\mathrm{E}[I]$.

B. Aggregate Interference

Departing from the assumption that the interference I caused by LoRa devices positioned over the l-th annulus is approximated by a gamma distribution with MGF $M_I^l(s) = (1-\theta_l s)^{-k_l}$, the MGF of the aggregate interference caused by the LoRa devices located in the circular region (L annuli) is given by

$$M_{I_{agg}}(s) = \prod_{l=1}^{L}(1-\theta_l s)^{-k_l}. \tag{17}$$

By considering the characteristic function of the aggregate interference power, represented as

$$\varphi_{I_{agg}}(t) = \prod_{l=1}^{L}(1-\theta_l it)^{-k_l}, \tag{18}$$

the PDF of the aggregate interference is computed by

$$f_{I_{agg}}(x) = \frac{1}{2\pi}\int_{-\infty}^{+\infty} e^{-itx}\varphi_{I_{agg}}(t)dt. \tag{19}$$

We highlight that the PDF of the aggregate interference in (19) can be efficiently computed by using the Fast Fourier Transform (FFT) algorithm, since the integral in (19) represents the Fourier Transform of the characteristic function. Finally, the CDF of the aggregate interference power can be computed as follows

$$F_{I_{agg}}(x) = \int_{-\infty}^{x} f_{I_{agg}}(z)dz. \tag{20}$$

IV. Model Accuracy

In this Section we compare numerical and simulation results of the aggregate interference power caused to the LoRa gateway. The LoRa network scenario considered in the comparison is the one represented in Fig. 1. LoRa devices are distributed over a circular region with a radius of approximately 12 kms, i.e., $R_1 = 20$ m and $R_{L+1} = 12020$ m. The devices must be compliant with the duty cycle limit imposed by the regulatory bodies. Due to this fact we have considered a duty cycle of 1% (imposed in Europe for sub-bands 863.0 - 868.0 MHz, 868.0 - 868.6 MHz, and 869.7 - 870.0 MHz), i.e. each device uses the spectrum at most 1% of the time. In our model the duty cycle is modeled by the access probability (τ), meaning that on average $n\tau$ devices are causing interference to the gateway. Simulation and numerical results are presented for two different densities of devices ($\{2\times10^{-2}, 2\times10^{-1}\}$ devices/m^2). Regarding the radio propagation, the path loss coefficient was parameterized to $\alpha = 4$ [15], while shadowing and Rayleigh were defined with $\sigma_\xi = 0.69$ and $\sigma_\zeta^2 = 0.5$, respectively. The parameters adopted to validate the distribution of the aggregate interference caused to the LoRa gateway are shown in Table I.

TABLE I
PARAMETERS ADOPTED IN THE SIMULATIONS.

R_1	20 m	R_{L+1}	12020 m
α	4	λ (node/m^2)	$\{2\times10^{-1}, 2\times10^{-2}\}$
σ_ξ	0.69	τ	$\{1\times10^{-2}, 5\times10^{-3}, 1\times10^{-3}\}$
ρ	20 m	P_{Tx}	14 dBm
L	600	σ_ζ^2	0.5

To assess the accuracy of the proposed model, we have computed the PDF and CDF of the interference caused to the LoRa gateway through (19) and (20), respectively. The PDF and CDF are compared with the empirical PDF and CDF obtained with the simulated data. To this purpose, we have run 1×10^6 simulations that consisted on determining the power received at the gateway due to the multiple transmissions of the LoRa devices. For each simulation we have considered a different realization of the devices' distribution, fading and shadowing power gain, and a selection of the transmitting devices according to the probability of transmission. In the model we considered $L = 600$ annuli of width $\rho = 20$ m.

The comparison of the CDF of the aggregate interference is illustrated in Fig. 2, assuming a spatial density of 2×10^{-2} devices/m^2 and for two probabilities of transmission ($\tau = 5\times10^{-3}$ and $\tau = 1\times10^{-2}$). It can be observed that the aggregate interference increases with the probability of transmission, as expected. Moreover, the numerical results (represented in the figure by the legend "Model") are close to the results obtained through simulation (represented in the figure by the legend "Simulation"). Similar results were obtained for different densities and transmission probabilities, indicating that the model is capable of presenting a good approximation of the empirical data. We have also validated the model considering a different number of annuli (L). For $L \geq 600$ the accuracy of the model remains constant and similar to the one presented in Fig. 2, indicating that no significant accuracy improvement is observed for $L \geq 600$.

Finally, we present the PDFs of the aggregate interference for three probabilities of transmission. The results, obtained with the model for $\lambda = 2\times10^{-1}$ devices/m^2, are presented in Fig. 3. As can be seen, non-gaussian distributions were obtained. Moreover, a different shape of the distribution is obtained for each probability of transmission, since the dominant interferers may impact differently on the aggregate interference.

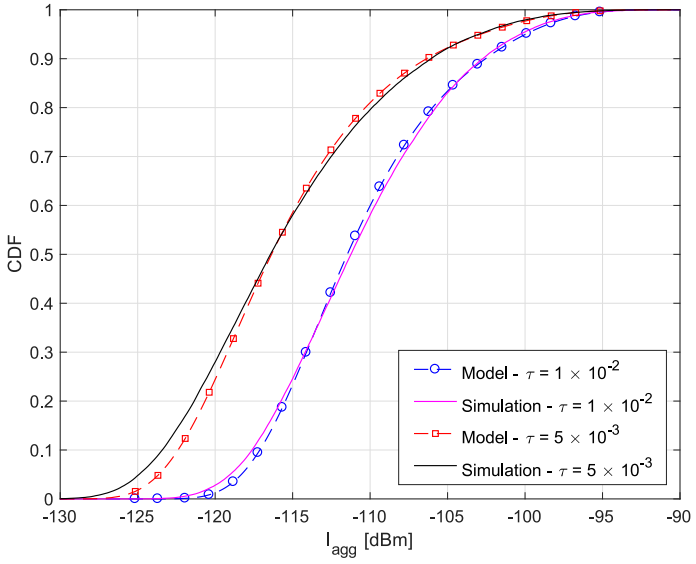

Fig. 2. CDF of aggregate interference power when LoRa devices transmit with probabilities $\tau = 1 \times 10^{-2}$ and $\tau = 5 \times 10^{-3}$.

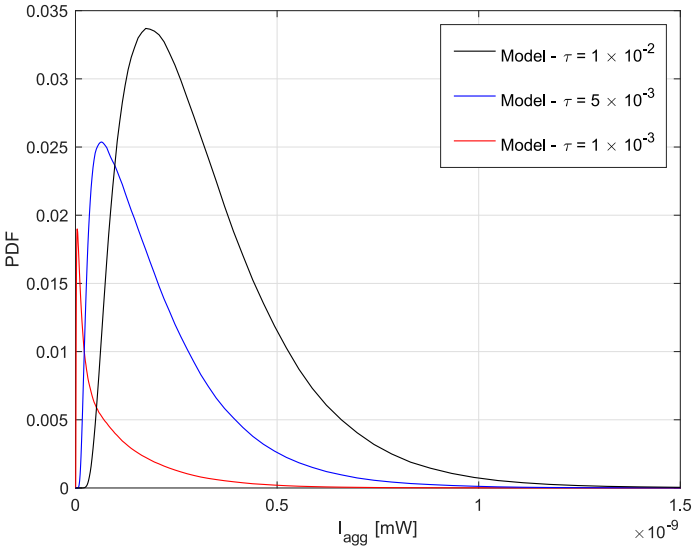

Fig. 3. Comparison of the aggregate interference PDF for different scenarios ($\lambda = 2 \times 10^{-1}$devices/m^2).

V. Conclusions

This work investigates the interference caused by multiple coexisting LoRa devices to a single gateway, when the LoRa devices are distributed according to a homogeneous PPP and considering path loss, fast fading, and shadowing effects. The distribution of the aggregate interference power was characterized, and a numerical approximation can be computed using the FFT algorithm. Different simulation results considering different channel access probabilities and densities of LoRa devices were compared with the numerical results, showing that the numerical CDF of the aggregate interference is close to the CDF obtained with the empirical data. The model presented in this paper is a first step to characterize the interference caused to a LoRa gateway and we believe that it is an important tool to better understand LoRa networks' performance and IoT networks in general.

Acknowledgements

This work is supported by the European Regional Development Fund (FEDER), through the Competitiveness and Internationalization Operational Programme (COMPETE 2020) of the Portugal 2020 and *Programa Operacional Regional LISBOA* (LISBOA 2020), and by national funds through *Fundação para a Ciência e Tecnologia* (FCT), under the projects CoSHARE (LISBOA-01-0145-FEDER-0307095 - PTDC/EEI-TEL/30709/2017), InfoCent-IoT (POCI-01-0145-FEDER-030433), project UID/EEA/50008/2019, and the grant SFRH/BD/108525/2015.

References

[1] U. Raza, P. Kulkarni, and M. Sooriyabandara, "Low Power Wide Area Networks: An Overview," *IEEE Commun. Surveys Tuts.*, vol. 19, no. 2, pp. 855–873, Secondquarter. 2017.

[2] TheThingsNetwork. Accessed Jan., 2019. [Online]. Available: https://www.thethingsnetwork.org

[3] Semtech. LoRa Modulation Basics. Accessed Jan., 2019. [Online]. Available: https://www.semtech.com

[4] LoRaWAN. LoRa Alliance. Accessed Jan., 2019. [Online]. Available: https://lora-alliance.org

[5] P. Neumann, J. Montavont, and T. Noël, "Indoor deployment of low-power wide area networks (LPWAN): A LoRaWAN case study," in *Proc. IEEE Int. Conf. on Wireless and Mobile Computing, Networking and Commun. (WiMob)*, New York, NY, USA, Oct. 2016, pp. 1–8.

[6] O. Iova, A. L. Murphy, G. P. Picco, L. Ghiro, D. Molteni, F. Ossi, and F. Cagnacci, "LoRa from the City to the Mountains: Exploration of Hardware and Environmental Factors," in *Proc. of the Int. Conf. on Embedded Wireless Systems and Networks*, 2017, pp. 317–322.

[7] O. Georgiou and U. Raza, "Low Power Wide Area Network Analysis: Can LoRa Scale?" *IEEE Wireless Commun. Lett.*, vol. 6, no. 2, pp. 162–165, Apr. 2017.

[8] A. Waret, M. Kaneko, A. Guitton, and N. E. Rachkidy, "LoRa Throughput Analysis with Imperfect Spreading Factor Orthogonality," *IEEE Wireless Commun. Lett.*, 2018.

[9] M. Abramowitz and I. A. Stegun, *Handbook of mathematical functions: with formulas, graphs, and mathematical tables*. Courier Corporation, 1965.

[10] Semtech. SX1272/73 - 860 MHz to 1020 MHz Low Power Long Range Transceiver, Datasheet. Accessed Jan., 2019. [Online]. Available: https://www.semtech.com/uploads/documents/sx1272.pdf

[11] A. Abdi and M. Kaveh, "On the utility of Gamma PDF in modeling shadow fading (slow fading)," in *Proc. IEEE Veh. Technol. Conf.*, Houston, TX, USA, May 1999, pp. 2308–2312.

[12] D. Lewinski, "Nonstationary probabilistic target and clutter scattering models," *IEEE Trans. Antennas Propag.*, vol. 31, no. 3, pp. 490–498, May 1983.

[13] S. Al-Ahmadi and H. Yanikomeroglu, "On the approximation of the Generalized-K distribution by a Gamma distribution for modeling composite fading channels," *IEEE Trans. Wireless Commun.*, vol. 9, no. 2, pp. 706–713, Feb. 2010.

[14] M. Haenggi and R. K. Ganti, "Interference in large wireless networks," *Foundations and Trends in Networking*, vol. 3, no. 2, pp. 127–248, Nov. 2009.

[15] D. Croce, M. Gucciardo, I. Tinnirello, D. Garlisi, and S. Mangione, "Impact of Spreading Factor Imperfect Orthogonality in LoRa Communications," in *Proc. of Digital Communication. Towards a Smart and Secure Future Internet*, 2017, pp. 165–179.